KSÜ Mühendislik Bilimleri Dergisi,28(2), 2025
Araştırma Makalesi

KSU J Eng Sci, 28(2), 2025
Research Article

Kahramanmaras Sutcu Imam University
Journal of Engineering Sciences

Geliş Tarihi : 13.01.2025
Kabul Tarihi :06.02.2025

Received Date : 13.01.2025
Accepted Date : 06.02.2025

SYNTHESIS OF POLYANILINE-BASED CATALYSTS: PHOTOCATALYTIC DEGRADATION OF METHYLENE BLUE

POLİANİLİN İÇERİKLİ KATALİZÖRLERİN SENTEZİ: METİLEN MAVİSİNİN FOTOKATALİTİK DEGRADASYONU

Nazli TURKTEN[1] (ORCID: 0000-0001-9343-3697)
Yunus KARATAS[1*] (ORCID: 0000-0002-3826-463X)
Yelda YALCIN GURKAN[2] (ORCID: 0000-0002-8621-2025)

[1] Department of Chemistry, Kirsehir Ahi Evran University, 40100, Kirsehir, Türkiye
[2] Department of Chemistry, Tekirdag Namik Kemal University, 59030, Tekirdag, Türkiye

*Sorumlu Yazar / Corresponding Author: Yunus KARATAS, ykaratas@ahievran.edu.tr

ABSTRACT

The increasing use of dyes in various industries has raised concerns regarding the potential release of harmful substances into the environment and their influence on human health. The incorporating style of polyaniline-based catalysts has attracted great interest in the field of photocatalysis, specifically for dye degradation from water. Polyaniline CuO (PANI-CuO) catalysts with varying PANI/CuO mole ratios (1:8, 1:1, and 8:1) were synthesized by *in-situ* chemical oxidation polymerization (PCI) and mechano-chemical preparation (PCS) methods. FTIR, XRD, and SEM analyses confirmed the presence of CuO and PANI in PCS catalysts. However, CuO particles were not detected in PCI specimens due to the dissolution of CuO in a highly acidic medium. The photocatalytic efficiency of prepared two different series of PANI-CuO catalysts was assessed by the degradation of methylene blue (MB) dye degradation for comparative purposes. The results implied that the preparation process significantly concerns the photocatalytic performance with PCI catalysts exhibiting higher MB photocatalytic degradation than PCS specimens. The PCI-18 specimen achieved 56% degradation of MB in 300 minutes.

Keywords: *In-situ* chemical oxidation polymerization, mechano-chemical preparation, methylene blue, PANI-CuO composites, photocatalysis.

ÖZET

Günümüzde boyalar birçok endüstride kullanılmakta olup, insan sağlığı üzerinde olumsuz etkileri olan zararlı maddelerin çevreye salınması endişe yaratmaktadır. Bu nedenle, polimer içerikli katalizörlerin hazırlanması ve sudan boyaların uzaklaştırılmasında kullanımı özellikle fotokataliz alanında büyük ilgi çekmektedir. Polianilin CuO (PANI-CuO) katalizörleri eş-anlı kimyasal oksidasyon polimerizasyonu (PCI) ve mekaniksel-kimyasal (PCS) olmak üzere iki farklı yöntem ile hazırlanmıştır. Bu yöntemlerde, PANI/CuO mol oranları (1:8, 1:1 ve 8:1) olacak şekilde kompozitler sentezlenmiştir. PCS katalizörlerinde, PANI ve CuO varlığı FTIR, XRD ve SEM analizleri kullanılarak saptanmıştır. Ancak, PCI örneklerinde yüksek asidik ortamda CuO çözünmesine bağlı olarak, CuO tanecikleri tespit edilememiştir. İki farklı seri olarak hazırlanan PANI-CuO katalizörlerinin fotokatalitik etkinliği, metilen mavisi (MB) kullanılarak, karşılaştırmalı olarak test edilmiştir. PCI katalizörlerinin MB boyasının fotokatalitik degradasyonunda PCS örneklerine kıyasla daha etkili olduğu gözlenmiştir. PCI-18 örneği kullanılarak, MB boyası %56 degradasyonuna 300 dakikada sonunda ulaşılmıştır.

Anahtar Kelimeler: Eş-anlı kimyasal oksidasyon polimerizasyonu, fotokataliz, mekaniksel-kimyasal hazırlama, metilen mavisi, PANI-CuO kompozitleri.

ToCite: TURKTEN, N., KARATAS, Y. & YALCIN GURKAN, Y., (2025). SYNTHESIS OF POLYANILINE-BASED CATALYSTS: PHOTOCATALYTIC DEGRADATION OF METHYLENE BLUE. *Kahramanmaraş Sütçü İmam Üniversitesi Mühendislik Bilimleri Dergisi*, 28(2), 851-862.

INTRODUCTION

With rapid growth and industrial development, extensive organic pollutants in manufacturing wastewater can pose a serious threat by being released into water bodies. Textile wastewater is one of the prominent environmental challenges due to its complex and diverse contaminants generated by textile manufacturing processes such as bleaching, dyeing, and sizing. Conventional treatment methods including biological and physical processes are inadequate to eliminate dyes. Consequently, comprehensive implementation of technology treatment is required to degrade various chemicals used in textile operations and solve secondary pollution issues. Advanced oxidation processes (AOPs) are chemical oxidation methods that use strong oxidants such as hydroxyl radicals, resulting in a non-selective reactivity with various organic pollutants. Furthermore, these methods generate hydroxylated or dehydrogenated products, which are then fragmented into smaller products (i.e., CO_2, H_2O, and inorganic ions). Among AOPs, photocatalysis is a promising sustainable method for dye removal from wastewater (Kallawar and Bhanvase, 2024; Khader et al., 2024; Khan et al., 2024). The photocatalytic mechanism for dye degradation proceeds under UV or visible light irradiation in the presence of a catalyst to generate electron/hole pairs. These pairs participate in redox reactions with adsorbed species on the photocatalyst surface, leading to the degradation of dyes into less harmless byproducts (Hoffmann et al., 1995; Khan et al., 2024).

Methylene blue (MB), one of the primary models of cationic dyes contains functional groups capable of dissociating into positively charged ions in an aqueous solution. MB is commonly used as a colorant in paper and textiles in the cotton dying process, also it is applied in pharmaceutical and self-care products. This dye can cause serious effects on humans, including increased heart rate, nausea, skin and eye irritation, and vomiting. Therefore, most articles have focused on various treatment techniques in the environmental remediation of MB (Lanjwani et al., 2024; Muzammal et al., 2024; Turkten et al., 2021b). Hence, up to now, numerous photocatalysts have been designed for the photocatalytic degradation of MB and further management is compulsory to remove MB using different catalysts (Khan et al., 2024; Lanjwani et al., 2024).

Recently, the design of conducting polymer-based catalysts has attracted great attention to reduce photogenerated electron/hole recombination and improve photocatalytic activity. Polyaniline (PANI) and its derivatives are among the most extensively studied conducting polymers coupled with semiconductor metal oxides used in photocatalytic applications for wastewater treatment (Sajith et al., 2024; Turkten et al., 2021a). In this regard, PANI-modified photocatalysts mostly combined with TiO_2 and ZnO semiconductors such as PANI-TiO_2 (Jangid et al., 2021; Rahman and Kar, 2020a, 2020b; Wang et al., 2010; Wang and Min, 2007; Yang et al., 2017), PANI-ZnO (Eskizeybek et al., 2012; Saravanan et al., 2016; Turkten et al., 2021b; Vijayalakshmi et al., 2021) have been prepared to remove MB and other synthetic dyes in wastewater. However, a few studies have been reported on the photocatalytic performance of PANI-CuO-based composites through the degradation of dyes and organic pollutants (Boucherdoud et al., 2024; Cui et al., 2024; Gelaw et al., 2022; Koysuren and Koysuren, 2023a,b; Nekooie et al., 2021; Rathore et al., 2020). Rathore and co-workers prepared chitosan-PANI-CuO nanocomposite using the batch adsorption method to remove methyl orange (Rathore et al., 2020). In another study, a series of boron-doped PANI-CuO composites was synthesized and photocatalytic degradation of MB was investigated (Koysuren and Koysuren, 2023a). The photocatalytic performances of PANI-CuO photocatalysts were studied on the degradation of MB (Boucherdoud et al., 2024), and MB dye and Cr(VI) (Koysuren and Koysuren, 2023b).

This research focused on a systematic kinetic study of the photocatalytic degradation of MB by prepared PANI-CuO composites via *in-situ* chemical oxidation polymerization and mechano-chemical methods. In addition to the limited studies reported on this subject in the literature, a systematic and comparative examination of these methods and the investigation of the structural and morphological differences depending on the preparation method by FTIR, XRD, and SEM analyses were aimed to fill an important gap in clarity.

MATERIALS AND METHODS

Materials

CuO, aniline (ANI), ammonium persulfate (APS), and HCl (37%), MB were purchased by Merck.

Preparation of PANI and PANI-CuO Composites

Polyaniline emeraldine salt (PANI) was prepared via *in-situ* chemical oxidation polymerization method, as described in our previous study (Turkten et al., 2023). CuO composites were synthesized by the mechano-chemical preparation method referred to as PCI composites and *in-situ* chemical oxidation polymerization method referred to as PCS composites as summarized as follows (Turkten et al., 2025). The mole ratios of PANI-CuO were 1:8, 1:1, and 8:1 and were named PCS-18, PCS-11, and PCS-81, respectively in PCS composites. Briefly, CuO and synthesized PANI (as described above) in 50 mL of distilled water stirred for 24 h. Then, the mixture was filtered and washed with distilled water. Finally, the solid product was dried at 80°C for 24 h. PCI composites were prepared at the initial ANI/CuO mole ratios of 1:8, 1:1, and 8:1 and were named PCI-18, PCI-11, and PCI-81, respectively. The initial mole ratio of ANI/APS was 1:1. Briefly, the representative synthesis of PCI-11 was given as follows: Firstly, 5.71 g (25 mmol) of APS was dissolved in 80 mL of 1 M HCl solution (Solution A). Solution B was obtained by adding 2.0 g (25 mmol) of CuO to 80 mL of 1 M HCl solution and ultrasonicated for 15 min. Then, 2.33 g (25 mmol) of ANI was added into Solution B which was placed in an ice bath. After that, Solution A was added dropwise into Solution B and stirred for another 24 h. Finally, the resulting product was filtered, washed, and dried at 80°C for 24 h.

Characterization

FTIR-ATR spectra were performed using a Thermo Scientific Nicolet 6700 Spectrometer. SEM analysis was carried out on a FEI-Philips XL30 Environmental Scanning Electron Microscope with an accelerating voltage of 10 kV. XRD data were acquired by a Rigaku-D/MAX-Ultima diffractometer (40 kV and 40 mA). Crystallite sizes (D, nm) of CuO, PCS, and PCI composites were determined by using the Scherrer equation (Equation 1) related to the (1 1 1) reflection plane of CuO (Scherrer, 1918).

$$D = K \lambda / (\beta \cos\theta) \quad (1)$$

K: 0.9, λ: 1.5418 Å, θ: Bragg angle, and β: full width at half maximum intensity (FWHM, radians).

Photocatalytic Activity Experiments

The photocatalytic activity of CuO nanoparticles was compared with two different series of PCS and PCI composites by observing the MB dye solution (10 mg/L) in the exposure time interval (t=0-300 min). A black-light fluorescent lamp (125 W) with a wavelength range of 300-420 nm at λ_{max}=365 nm was used in experiments. The suspension in the cylindrical Pyrex reaction vessel was prepared by adding an optimum amount of photocatalyst (0.25 mg/L) in a 50 mL MB solution. After that, the suspension was filtered at certain photocatalytic time intervals, followed by UV-vis analysis. The percent removal of MB dye was calculated using Equation (2).

$$\text{Decolorization, \%} = ((A_o - A) / A_{,o}))x100 \quad (2)$$

A_o: initial absorbance of MB dye
A_t: absorbance of MB dye at time t.

RESULTS AND DISCUSSION

Characterization of Photocatalysts

Characterization of PANI, CuO, PCS, and PCI specimens was reported previously and summarized as follows (Turkten et al., 2025). The main FTIR peaks of PANI were observed at 1585 cm^{-1} and 1481 cm^{-1} for the C=N and C=C stretching modes of the quinonoid and benzenoid rings, respectively (Deng et al., 2016) (Figure 1 (a)). The characteristic peak occurring at 1296 cm^{-1} was attributed to the C-N stretching mode of the aromatic amine structure. The peak at 1242 cm^{-1} was ascribed to the conducting protonated form of the polymer indicating the presence of C–$N^{+\bullet}$ stretching vibration in the polaron structure. The intense peak at 1110 cm^{-1} could belong to a vibrational mode of either B–NH^{+}=Q or B–$NH^{+\bullet}$–B (B: benzenoid, Q: quinone) charged units formation due to the protonation process (Ping, 1996; Trchová and Stejskal, 2011). The peaks in the 900 cm^{-1}-700 cm^{-1} region (at 818 cm^{-1} and 797 cm^{-1}) corresponded to the aromatic-ring and out-of-plane C–H deformation vibrations (Stejskal and Sapurina, 2008). The three characteristic peaks of monoclinic CuO observed at 594 cm^{-1}, 523 cm^{-1}, and 470 cm^{-1} were related to the stretching modes of the metal-oxygen (Cu-O) bond (Figures 1 (b) and (c)). A weak peak located at 1651 cm^{-1} belonging to the bending vibration (O-H group) of absorbed water on the surface (Borgohain et al., 2000). It could be seen from the FTIR spectra of PCS composites that the characteristic peaks of both PANI and CuO nanoparticles were exhibited in Figure 1 (b). The peaks belonging to PANI at 1585 cm^{-1} and 1481 cm^{-1} shifted to blue due to the

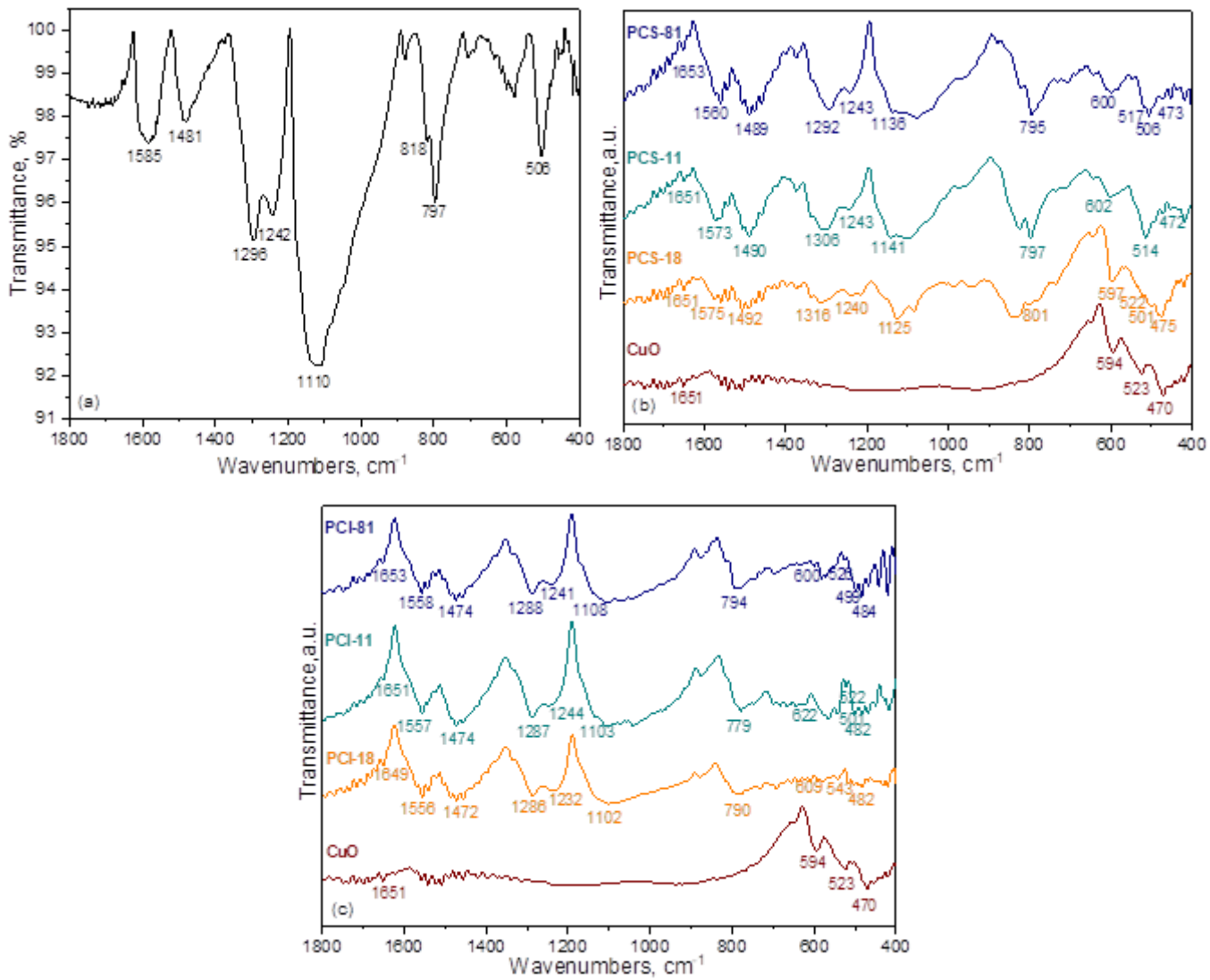

Figure 1. FTIR spectra of (a) PANI, (b) CuO and PCS-composites (c) CuO and PCI-composites.

electrostatic interaction between a charged structure of PANI and CuO nanoparticles in the spectrum of the PCS-81 composite, respectively (Singh and Shukla, 2020). For PCS-81 composite, the peaks at 1292 cm^{-1}, 1243 cm^{-1}, 1136 cm^{-1}, 795 cm^{-1}, and 506 cm^{-1} were ascribed to PANI while the peaks observed at 600 cm^{-1}, 517 cm^{-1}, and 473 cm^{-1} related to CuO. Depending on the increased amount of CuO, the quinonoid and benzenoid ring peaks corresponding to the backbone of PANI shifted, and their intensities also diminished gradually. All PCI composites revealed peaks only representing PANI that differed or changed in peak locations and intensities (Figure 1 (c)). The absence of CuO vibration signals was attributed to the instability of CuO in a highly acidic environment resulting in the dissolution of CuO and releasing Cu^{2+} ions (Fu et al., 2024; Turkten et al., 2025).

The XRD diffractograms of PANI, CuO, PCS-PANI, and PCI-PANI specimens are presented in Figure 2. The peaks of PANI at 2θ = 8.99º, 15.42º, 20.34º, 25.30º, and 27.18º could belong to the (0 0 1), (0 1 1), (0 2 0), (2 0 0), and (1 2 1) reflection semicrystalline planes, respectively (Jaroslav Stejskal et al., 1998).

The XRD diffractogram of CuO exhibited peaks at 2θ = 32.54°, 35.56°, 38.72°, 48.80°, 53.36°, 58.32°, 61.56°, 65.84°, 66.30°, 68.12°, 72.44°, and 75.02° corresponding to (1 1 0), (−1 1 1), (1 1 1), (−2 0 2), (0 2 0), (2 0 2), (−1 1 3), (0 2 2), (−3 1 1), (2 2 0), (3 1 1) and (0 0 4) planes of monoclinic CuO (JCPDS card no. 89-5895) (Devi et al., 2017).

The diffractogram of the PCS-81 and PCS-11 composites revealed semicrystalline PANI and crystalline monoclinic peaks of CuO with a slight spectral shift. The intensity of the PANI peaks decreased substantially depending upon

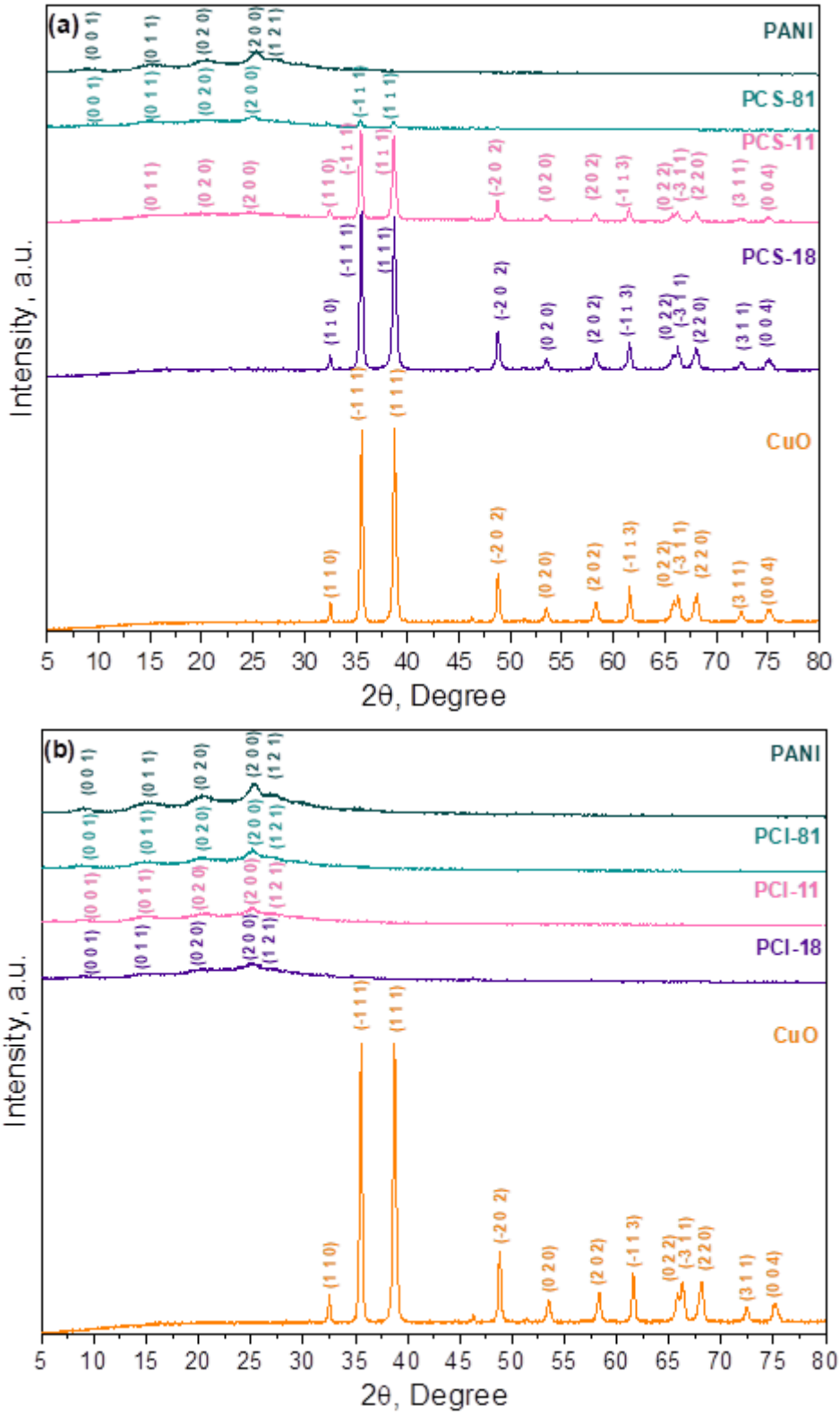

Figure 2. XRD diffractograms for (a) PANI, PCS-PANI composites, and CuO, (b) PANI, PCI-PANI composites, and CuO.

an increase in CuO amount in composites, while all semicrystalline peaks representing PANI disappeared in the PCS-18 composite as expected. However, XRD diffractograms of PCI composites presented only semicrystalline planes associated with PANI. The absence of characteristic reflections corresponding to CuO was a sign of CuO dissolution in a highly acidic medium and this finding was consistent with FTIR analysis.

The calculated crystallite size values of CuO, PCS-81, PCS-11, and PCS-18 specimens were 26 nm, 25 nm, 24 nm, and 23 nm respectively.

SEM images of PANI, CuO, PCS-PANI, and PCI-PANI specimens are presented in Figure 3. PANI revealed large globular-like structures, whereas CuO particles comprise various polyhedral forms. It was observed that the dominant morphology changed from PANI to CuO and the agglomeration tendency increased due to the increasing CuO amount in PCS composites. SEM images corresponded to PCI-81 and PCI-11 maintained the only typical PANI matrix although a loose cotton-like structure was observed in PCI-18 composite as reported in the literature (Ullah et al., 2014). The reason for this noticeable surface modification could be the change in coordination geometry of transition metal ion Cu^{2+} originated from the dissolution of CuO (Pandey et al., 2015). SEM results were consistent with the previously discussed FTIR and XRD analyses.

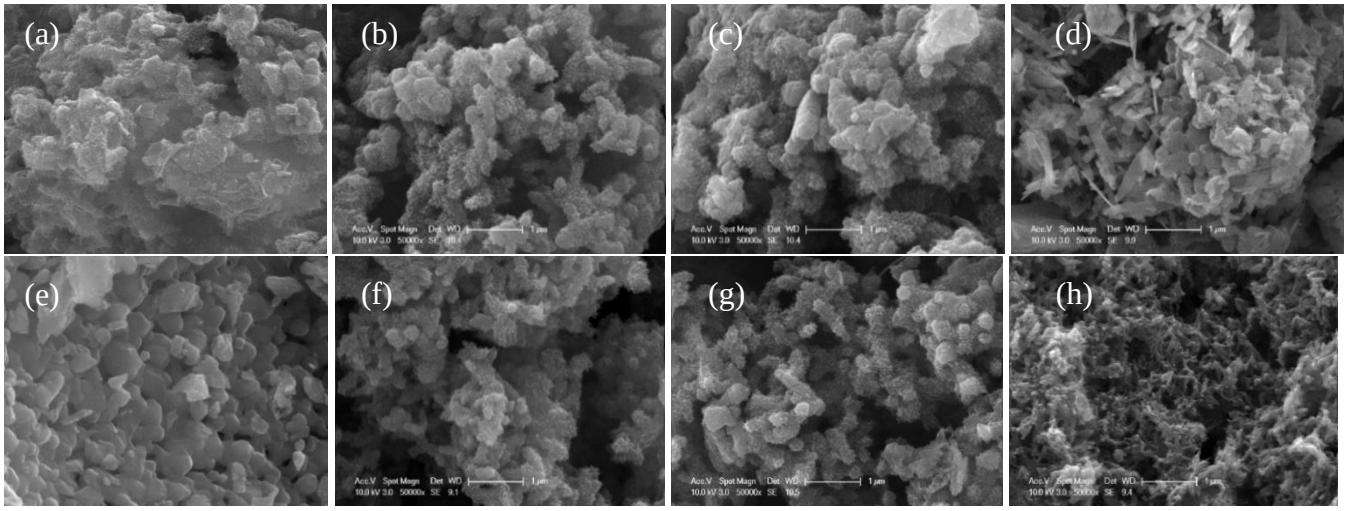

Figure 3. SEM x50000 of (a) PANI, (b) PCS-81, (c) PCS-11, (d) PCS-18, (e) CuO, (f) PCI-81, (g) PCI-11, and (h) PCI-18.

Photocatalytic Activity

MB was chosen as a model dye component to evaluate the photocatalytic performance of CuO nanoparticles, PCS, and PCI composites. The time-dependent UV-vis spectral features of MB (10 mg/L, referred to initial) during 0-300 min exposure are presented in Figures 4 and 5.

The aqueous solution of MB without the catalyst revealed a maximum absorption band at λ_{max}=664 nm, related to the conjugation system involving two dimethylamine-substituted aromatic rings through sulfur and nitrogen atoms. The observed shoulder at λ=613 nm corresponded to the dimmer of MB dye. The bands observed at λ=246 nm and λ=292 nm in the UV region were assigned to the substituted benzenes rings (Rauf et al. 2010). In all cases, the characteristic absorption bands of MB at λ_{max}=664 nm and λ=613 nm decreased with the progress of MB degradation reaction and irradiation time.

A comparison was made between the degree of MB decolorization in the presence of CuO nanoparticles, PCS, and PCI composites (Figure 6) and the corresponding data reported in Table 1.

The degree of MB decolorization in the presence of CuO was 56% after 300 min UV irradiation, which was in accordance with the literature (Shanmugam et al. 2023). The point of zero charge(pH_{pzc}) is an important parameter for predicting the surface charge of the photocatalyst based on the electrostatic interactions between MB and CuO surfaces related to photocatalytic efficiency. The pH_{pzc} value of CuO was reported as ~8.5 (Khan et al. 2019), whereas the pKa value of the cationic dye MB was 3.8 (Poorsajadi et al. 2022). Since the working solution was at around pH=5.5, pH_{pzc}>pH, the surface of CuO was positively charged, and the cationic MB dye with $C–S^{+}=C$ functional group was expected to be repelled away from the positively charged surface of CuO. This was also the case for similar catalyst-dye systems reported (Trandafilović et al. 2017). Interestingly, the PCI-18 composite revealed effective photodegradation compared to CuO and the other composites.

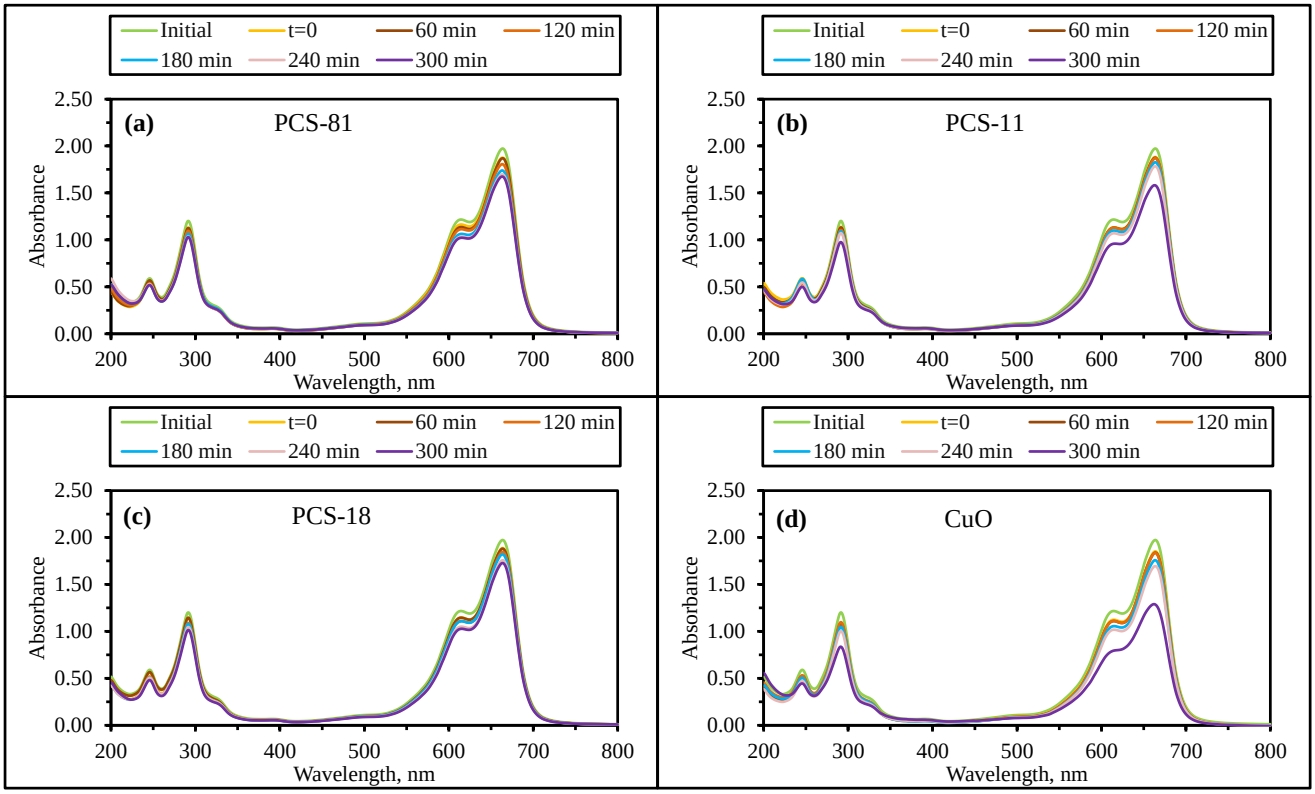

Figure 4. UV-vis spectral features of MB using (a) PCS-81, (b) PCS-11, (c) PCS-18, and (d) CuO.

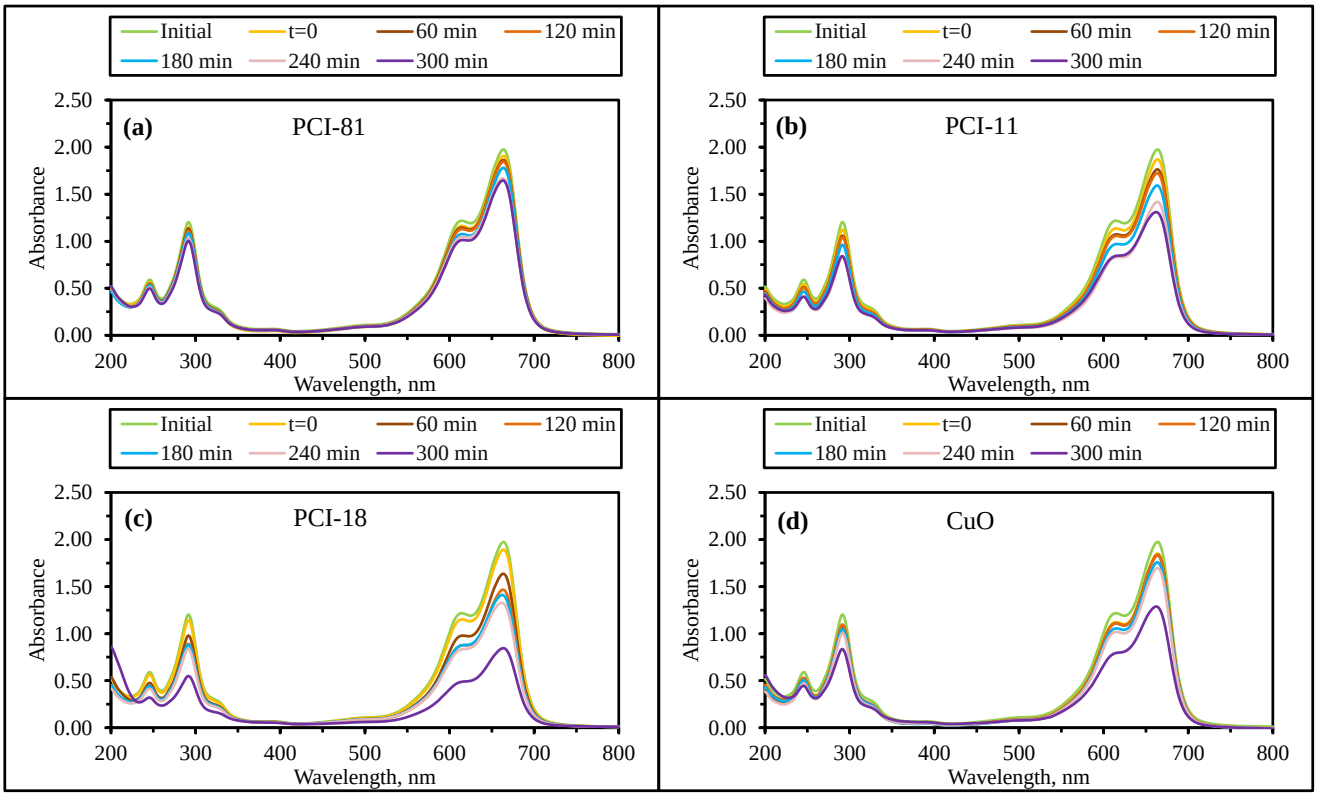

Figure 5. UV-vis spectral features of MB using (a) PCI-81, (b) PCI-11, (c) PCI-18, and (d) CuO.

Indeed, in the presence of PCI-18, approximately 56% of MB was degraded after 300 min, with a lower photocatalytic efficiency (36%) in the case of CuO, and an even smaller value was obtained for the other composites. The morphology, crystalline structure, and dimensions of catalysts played a vital role in photocatalytic activity (Dulta et

al. 2022). The increase in the removal efficiency of MB could be explained by the surface fiber-like, i.e. loose morphology resulting in the considerably high surface area of PCI-18 presented in SEM (Figure 3 (h)).

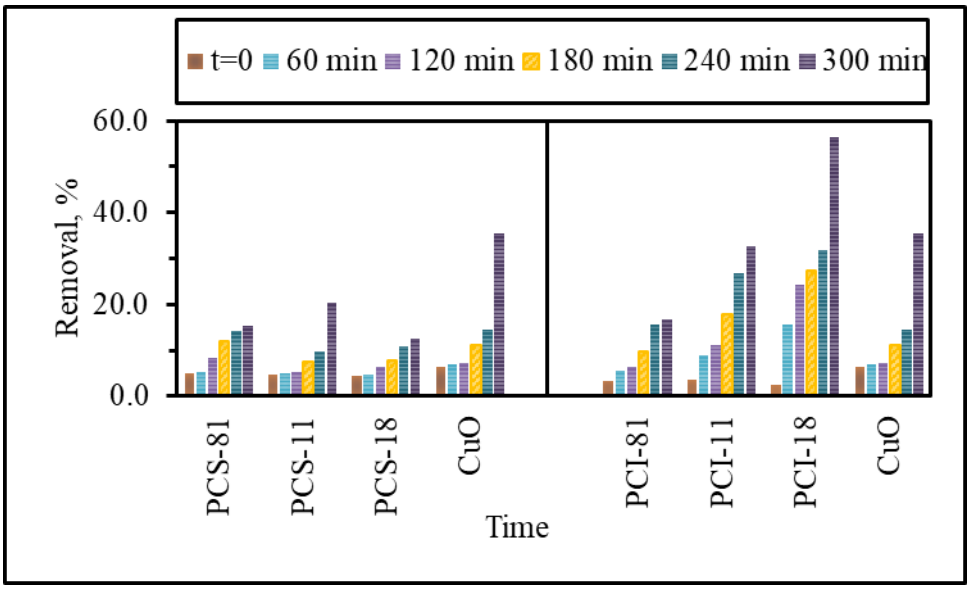

Figure 6. Photocatalytic degradation of MB in the presence of CuO particles, PCS, and PCI composites.

Table 1. Photocatalytic Degradation of MB in the Presence of CuO Particles, PCS, and PCI Composites

	Removal % at time t				
Specimens	**60 min**	**120 min**	**180 min**	**240 min**	**300 min**
CuO	6.99	7.24	11.2	14.4	35.6
PCS-81	5.33	8.51	12.0	14.1	15.3
PCS-11	5.09	5.39	7.56	9.82	20.4
PCS-18	4.80	6.53	7.84	11.0	12.5
PCI-81	5.66	6.54	9.83	15.7	16.8
PCI-11	9.06	11.1	17.9	26.8	32.8
PCI-18	15.6	24.4	27.5	31.9	56.4

As evidenced by spectral features (Figures 4 and 5), the photocatalytic degradation of MB using CuO nanoparticles and PANI-CuO composites following the pseudo-first-order kinetics model expressed by Equation 3.

$$\text{Rate } (R) = -dA/dt = kA \quad (3)$$

R: pseudo-first-order rate, $cm^{-1}min^{-1}$,
A_o: initial absorbance of MB,
A: absorbance of MB at time t,
t: irradiation time, min,
k: pseudo-first-order reaction rate constant, min^{-1}.

Half-life ($t_{1/2}$, min) could easily be calculated by the following equation, $t_{1/2}=0.692/k$.
The related kinetic parameters ($R^2>0.75$) are presented in Table 2.

Table 2. The Kinetic Parameters of CuO Particles, PCS, and PCI Composites

	First-order kinetic parameters		
Specimens	**kx10^{-4}, min^{-1}**	**$t_{1/2}$, min**	**Rate, cm^{-1} min^{-1}**
CuO	11.6	598	0.00229
PCS-18	5.50	1260	0.00109
PCS-11	6.10	1136	0.00120
PCS-81	4.20	1650	0.00083
PCI-81	6.10	1136	0.00120
PCI-11	13.4	517	0.00264
PCI-18	23.5	295	0.00464

On comparing the photocatalytic degradation results of all PCI and PCS specimens, the photocatalytic degradation rate constants could be described as:

PCI-18>PCI-11>CuO>PCI-81=PCS-11>PCS-18>PCS-81

The highest decolorization rate constant was observed when PCS-11 was used among PCS composites and PCI-18 was used among PCI composites. The rate constants obtained for PCI-18 and CuO specimens were k=23.5x10$^{-4.}$ min^{-1} and k=11.6x10$^{-4.}$ min^{-1}, respectively. This finding indicated that the photocatalytic activity of PCI-18 was about two times higher than that of CuO. The reason could be related to the loose cotton-like structure of the PCI-18 composite as seen in the SEM image.

CONCLUSION

The photocatalytic properties of PANI-CuO composites, affected by the synthesis method in terms of structural and morphological differences, were investigated by a comparative kinetic study. FTIR spectra of PCS composites presented the characteristic vibrations, belonging to PANI and CuO that differed or changed in peak locations and intensities, while the peaks of CuO were missing in PCI composites. Additionally, XRD analysis revealed that only characteristic planes corresponding to PANI were observed in PCI composites. The photocatalytic performances of CuO and PANI-CuO composites were studied in the degradation of a cationic MB dye. UV-vis intensities of characteristic bands belonging to MB gradually decreased in the presence of photocatalysts. It is well-known that morphology, crystalline structure, and dimensions play a crucial role in photocatalytic activity. PCI-18 composite achieved a satisfactory degradation efficiency of MB (56%), revealing a loose cotton-like structure derived from the dissolution of CuO.

REFERENCES

Borgohain, K., Singh, J. B., Rama Rao, M. V., Shripathi, T., & Mahamuni, S. (2000). Quantum size effects in CuO nanoparticles. *Physical Review B, 61*(16), 11093-11096. doi:10.1103/PhysRevB.61.11093

Boucherdoud, A., Kherroub, D. E., Dahmani, K., Douinat, O., Seghier, A., Bestani, B., & Benderdouche, N. (2024). Polyaniline/cupric oxide organometallic nanocomposites as a sonocatalyst for the degradation of methylene blue: Experimental study, RSM optimization, and DFT analysis. *Journal of Organometallic Chemistry, 1022*, 123386. doi:https://doi.org/10.1016/j.jorganchem.2024.123386

Cui, Z., Yuan, R., Chen, H., Zhou, B., Zhu, B., & Zhang, C. (2024). Application of polyaniline-based photocatalyst in photocatalytic degradation of micropollutants in water: A review. *Journal of Water Process Engineering, 59*, 104900. doi:https://doi.org/10.1016/j.jwpe.2024.104900

Deng, Y., Tang, L., Zeng, G., Dong, H., Yan, M., Wang, J., Hu, W., Wang, J., Zhou, Y., & Tang, J. (2016). Enhanced visible light photocatalytic performance of polyaniline modified mesoporous single crystal TiO_2 microsphere. *Applied Surface Science, 387*, 882-893. doi:https://doi.org/10.1016/j.apsusc.2016.07.026

Devi, L. V., Selvalakshmi, T., Sellaiyan, S., Uedono, A., Sivaji, K., & Sankar, S. (2017). Effect of La doping on the lattice defects and photoluminescence properties of CuO. *Journal of Alloys and Compounds, 709*, 496-504. doi:https://doi.org/10.1016/j.jallcom.2017.03.148

Eskizeybek, V., Sarı, F., Gülce, H., Gülce, A., & Avcı, A. (2012). Preparation of the new polyaniline/ZnO nanocomposite and its photocatalytic activity for degradation of methylene blue and malachite green dyes under UV and natural sun lights irradiations. *Applied Catalysis B: Environmental, 119-120*, 197-206. doi:10.1016/j.apcatb.2012.02.034

Fu, H., Shewfelt, S., Sylvan, L. D., Gaillard, J.-F., & Gray, K. A. (2024). Polyaniline-metal oxide coatings for biocidal applications: Mechanisms of activation and deactivation. *Chemosphere, 346*, 140543. doi:https://doi.org/10.1016/j.chemosphere.2023.140543

Gelaw, T. B., Sarojini, B. K., & Kodoth, A. K. (2022). Chitosan/Hydroxyethyl Cellulose Gel Immobilized Polyaniline/CuO/ZnO Adsorptive-Photocatalytic Hybrid Nanocomposite for Congo Red Removal. *Journal of Polymers and the Environment, 30*(10), 4086-4101. doi:10.1007/s10924-022-02492-4

Hoffmann, M. R., Martin, S. T., Choi, W., & Bahnemann, D. W. (1995). Environmental Applications of Semiconductor Photocatalysis. *Chemical Reviews, 95*(1), 69-96. doi:10.1021/cr00033a004

Jangid, N. K., Jadoun, S., Yadav, A., Srivastava, M., & Kaur, N. (2021). Polyaniline-TiO_2-based photocatalysts for dyes degradation. *Polymer Bulletin, 78*(8), 4743-4777. doi:10.1007/s00289-020-03318-w

Kallawar, G. A., & Bhanvase, B. A. (2024). A review on existing and emerging approaches for textile wastewater treatments: challenges and future perspectives. *Environmental Science and Pollution Research, 31*(2), 1748-1789. doi:10.1007/s11356-023-31175-3

Khader, E. H., Muslim, S. A., Saady, N. M. C., Ali, N. S., Salih, I. K., Mohammed, T. J., Albayati, T.M., & Zendehboudi, S. (2024). Recent advances in photocatalytic advanced oxidation processes for organic compound degradation: A review. *Desalination and Water Treatment, 318*, 100384. doi:https://doi.org/10.1016/j.dwt.2024.100384

Khan, S., Noor, T., Iqbal, N., & Yaqoob, L. (2024). Photocatalytic Dye Degradation from Textile Wastewater: A Review. *ACS Omega, 9*(20), 21751-21767. doi:10.1021/acsomega.4c00887

Koysuren, H. N., & Koysuren, O. (2023a). Photocatalytic Activity of Boron Doped CuO and Its Composite with Polyaniline. *Polymer-Plastics Technology and Materials, 62*(3), 281-293. doi:10.1080/25740881.2022.2113894

Koysuren, O., & Koysuren, H. N. (2023b). Application of CuO and its composite with polyaniline on the photocatalytic degradation of methylene blue and the Cr(VI) photoreduction under visible light. *Journal of Sol-Gel Science and Technology, 106*(1), 131-148. doi:10.1007/s10971-023-06049-2

Lanjwani, M. F., Tuzen, M., Khuhawar, M. Y., & Saleh, T. A. (2024). Trends in photocatalytic degradation of organic dye pollutants using nanoparticles: A review. *Inorganic Chemistry Communications, 159*, 111613. doi:https://doi.org/10.1016/j.inoche.2023.111613

Muzammal, S., Ahmad, A., Sheraz, M., Kim, J., Ali, S., Hanif, M. B., Hussain, I., Pandiaraj S., Alodhayb, A., Javed, M.S., Al-bonsrulah, H.A.Z., & Motola, M. (2024). Polymer-supported nanomaterials for photodegradation: Unraveling the methylene blue menace. *Energy Conversion and Management: X, 22*, 100547. doi:https://doi.org/10.1016/j.ecmx.2024.100547

Nekooie, R., Shamspur, T., & Mostafavi, A. (2021). Novel CuO/TiO_2/PANI nanocomposite: Preparation and photocatalytic investigation for chlorpyrifos degradation in water under visible light irradiation. *Journal of Photochemistry and Photobiology A: Chemistry, 407*, 113038. doi:https://doi.org/10.1016/j.jphotochem.2020.113038

Pandey, K., Yadav, P., & Mukhopadhyay, I. (2015). Elucidating the effect of copper as a redox additive and dopant on the performance of a PANI based supercapacitor. *Physical Chemistry Chemical Physics, 17*(2), 878-887. doi:10.1039/C4CP04321A

Ping, Z. (1996). In situ FTIR–attenuated total reflection spectroscopic investigations on the base–acid transitions of polyaniline. Base–acid transition in the emeraldine form of polyaniline. *Journal of the Chemical Society, Faraday Transactions, 92*(17), 3063-3067. doi:10.1039/FT9969203063

Rahman, K. H., & Kar, A. K. (2020a). Effect of band gap variation and sensitization process of polyaniline (PANI)-TiO_2 p-n heterojunction photocatalysts on the enhancement of photocatalytic degradation of toxic methylene blue with UV irradiation. *Journal of Environmental Chemical Engineering, 8*(5), 104181. doi:https://doi.org/10.1016/j.jece.2020.104181

Rahman, K. H., & Kar, A. K. (2020b). Titanium-di-oxide (TiO_2) concentration-dependent optical and morphological properties of PAni-TiO_2 nanocomposite. *Materials Science in Semiconductor Processing, 105*, 104745. doi:https://doi.org/10.1016/j.mssp.2019.104745

Rathore, B. S., Chauhan, N. P. S., Rawal, M. K., Ameta, S. C., & Ameta, R. (2020). Chitosan–polyaniline–copper(II) oxide hybrid composite for the removal of methyl orange dye. *Polymer Bulletin, 77*(9), 4833-4850. doi:10.1007/s00289-019-02994-7

Sajith, M., S, H., & Sambhudevan, S. (2024). A Comprehensive Review on Photocatalytic Degradation of Textile Dyes Using PANI-Semiconductor Composites. *Water, Air, & Soil Pollution, 235*(9), 594. doi:10.1007/s11270-024-07399-5

Saravanan, R., Sacari, E., Gracia, F., Khan, M. M., Mosquera, E., & Gupta, V. K. (2016). Conducting PANI stimulated ZnO system for visible light photocatalytic degradation of coloured dyes. *Journal of Molecular Liquids, 221*, 1029-1033. doi:https://doi.org/10.1016/j.molliq.2016.06.074

Scherrer, P. (1918). Estimation of the size and internal structure of colloidal particles by means of röntgen. *Nachrichten von der Gesellschaft der Wissenschaften zu Göttingen, 2*, 96–100.

Singh, P., & Shukla, S. K. (2020). Structurally optimized cupric oxide/polyaniline nanocomposites for efficient humidity sensing. *Surfaces and Interfaces, 18*, 100410. doi:https://doi.org/10.1016/j.surfin.2019.100410

Stejskal, J., Riede, A., Hlavatá, D., Prokeš, J., Helmstedt, M., & Holler, P. (1998). The effect of polymerization temperature on molecular weight, crystallinity, and electrical conductivity of polyaniline. *Synthetic Metals, 96*(1), 55-61. doi:10.1016/s0379-6779(98)00064-2

Stejskal, J., & Sapurina, I. (2008). Polyaniline — A Conducting Polymer. In U. Schubert, N. Hüsing, & R. M. Laine (Eds.), *Materials Syntheses: A Practical Guide* (pp. 199-207). Vienna: Springer Vienna.

Trchová, M., & Stejskal, J. (2011). Polyaniline: The infrared spectroscopy of conducting polymer nanotubes (IUPAC Technical Report). *Pure and Applied Chemistry, 83*(10), 1803-1817. doi:doi:10.1351/PAC-REP-10-02-01

Turkten, N., Karatas, Y., & Bekbolet, M. (2021a). Conducting Polymers and Photocatalysis: A Mini Review on Selected Conducting

Polymers and Photocatalysts as TiO_2 and ZnO. *Journal of Photocatalysis, 2*(4), 252-270. doi:10.2174/2665976x02666211201121530

Turkten, N., Karatas, Y., & Bekbolet, M. (2021b). Preparation of PANI Modified ZnO Composites via Different Methods: Structural, Morphological and Photocatalytic Properties. *Water, 13*(8). doi:10.3390/w13081025

Turkten, N., Karatas, Y., Uyguner-Demirel, C. S., & Bekbolet, M. (2023). Preparation of PANI modified TiO_2 and characterization under pre- and post- photocatalytic conditions. *Environmental Science and Pollution Research, 30*(51), 111182-111207. doi:10.1007/s11356-023-30090-x

Turkten, N., Karatas, Y., & Yalcin Gurkan, Y. (2025). New Insights into the Application of Copper-Based Polymer Composites: A Depth Experimental and Computational *Inorganic Chemistry Communications*.

Ullah, R., Bilal, S., Ali, K., & Shah, A.-u.-H. A. (2014). Synthesis and characterization of polyaniline doped with Cu II chloride by inverse emulsion polymerization. *Synthetic Metals, 198*, 113-117. doi:https://doi.org/10.1016/j.synthmet.2014.09.024

Vijayalakshmi, S., Kumar, E., Ganeshbabu, M., Venkatesh, P. S., & Rathnakumar, K. (2021). Structural, electrical, and photocatalytic investigations of PANI/ZnO nanocomposites. *Ionics, 27*(7), 2967-2977. doi:10.1007/s11581-021-04041-w

Wang, F., Min, S., Han, Y., & Feng, L. (2010). Visible-light-induced photocatalytic degradation of methylene blue with polyaniline-sensitized TiO_2 composite photocatalysts. *Superlattices and Microstructures, 48*(2), 170-180. doi:https://doi.org/10.1016/j.spmi.2010.06.009

Wang, F., & Min, S. X. (2007). TiO_2/polyaniline composites: An efficient photocatalyst for the degradation of methylene blue under natural light. *Chinese Chemical Letters, 18*(10), 1273-1277. doi:https://doi.org/10.1016/j.cclet.2007.08.010

Yang, C., Dong, W., Cui, G., Zhao, Y., Shi, X., Xia, X., Tang, B., & Wang, W. (2017). Enhanced photocatalytic activity of PANI/TiO_2 due to their photosensitization-synergetic effect. *Electrochimica Acta, 247*, 486-495. doi:https://doi.org/10.1016/j.electacta.2017.07.037